Indian Journal of Marine Sciences
Vol. 15, March 1986, pp. 8-12

Numerical Model for Wind-driven Circulation in the Bay of Bengal*

N BAHULAYAN & V V R VARADACHARI
National Institute of Oceanography, Dona Paula, Goa 403 004

Received 3 *May* 1984; *revised received* 30 *October* 1985

Wind-driven circulation in the Bay of Bengal, generated by a southwest wind of constant speed (10 m . sec^{-1}) and direction (225° TN), is presented. A non-linear hydrodynamic model is used for the simulation of circulation. Numerical experiments have shown that when a uniform wind stress is suddenly imposed over the sea surface, a steady circulation is generated after 50 h of numerical integration of model equations. The sensitivity of this model to bathymetry and coastal configuration is also discussed. The study shows that maximum current speed is observed near the coastal region as anticipated and it generally tends to follow the idealised bottom contours.

Lighthill[1] studied the dynamic response of the Indian Ocean to the onset of southwest monsoon by means of an analytical model. Later, Cox[2] studied the currents and water masses of the Indian Ocean utilising a 3 dimensional numerical model where seasonal reversal of currents were simulated. However, the peculiarities of circulation in the Bay of Bengal could not be extracted probably due to the coarse grid used in that model. Models of this kind were developed and used with considerable success to study the hydrodynamics of large variety of bays and seas[3-10].

The principal objective of this work is to simulate the wind-driven circulation in the Bay of Bengal using a depth averaged hydrodynamical-numerical model[11] in which a constant southwesterly wind is used as input. The variation of coriolis parameter with latitude and an idealised bottom topography are taken into account. Intrusion of river waters into the Bay is restricted by the resolution of the model.

Methods

Model equations—A system of rectangular cartesian coordinates with x, y and z axis pointing east, north and vertically upward directions respectively, is considered. The displaced level of sea surface is given by $z=\zeta(x, y, t)$ and the sea floor corresponds to $z=-h(x, y)$.

The depth averaged dynamical equations used to describe barotropic motion of a homogeneous ocean on a β-plane are

$$\frac{\partial u}{\partial t}+u\frac{\partial u}{\partial x}+v\frac{\partial u}{\partial y}-fv = -g\left(\frac{\partial \zeta}{\partial x}\right)+\frac{1}{(\zeta+h)}\left[\frac{\tau_x^{\zeta}}{\rho_w}-ku(u^2+v^2)^{1/2}\right] \quad \ldots(1)$$

$$\frac{\partial v}{\partial t}+u\frac{\partial v}{\partial x}+v\frac{\partial v}{\partial y}+fu = -g\left(\frac{\partial \zeta}{\partial y}\right)+\frac{1}{(\zeta+h)}\left[\frac{\tau_y^{\zeta}}{\rho_w}-kv(u^2+v^2)^{1/2}\right] \quad \ldots(2)$$

and the equation of continuity in the vertically integrated form as

$$\frac{\partial \zeta}{\partial t}+\frac{\partial}{\partial x}[(\zeta+h)u]+\frac{\partial}{\partial y}[(\zeta+h)v]=0 \quad \ldots(3)$$

The bottom stress in Eqs 1 and 2 is parameterised in terms of a quadratic friction law.

Eqs 1 and 2 have been transformed to flux form as shown below (Eqs 4 and 5) for convenience and form the basis for the numerical solution, together with Eq. 3.

Symbols used: ζ = elevations of sea surface with reference to its undisturbed state; f = coriolis parameter which is assumed to vary linearly with latitude ($f=f_0+\beta y$); $\beta=\frac{\partial f}{\partial y}$; g – acceleration due to gravity; ρ_w, ρ_a = density of water and air respectively; h = depth of seabed from undisturbed sea surface; u, v = zonal and meridional component of depth averaged velocities defined by

$$u=\frac{1}{(\zeta+h)}\int_{-h}^{\zeta}u'\,dz \quad \text{and} \quad v=\frac{1}{(\zeta+h)}\int_{-h}^{\zeta}v'\,dz$$

where u' and v' are horizontal velocity components in respective directions at a depth z from the sea surface; τ_x^{ζ}, τ_y^{ζ} = x and y components of surface wind stress; i, j – indices to represent space coordinates of grid points defined by $x_i=(i-1)\Delta x$ and $y_j=(j-1)\Delta y$, where $i=1, 2\ldots m$ and $j=1, 2\ldots n$ and Δx and Δy are small increments in x and y; p = index to represent time step in numerical integration ($t=t_p=p\Delta t$ where $p=0, 1, 2\ldots$); k = bottom friction coefficient (2.6×10^{-3}); C_D = drag coefficient of air at the sea surface (2.8×10^{-3}); u_a = x-component of velocity of wind at 10 m above sea surface; and v_a = y-component of velocity of wind at 10 m above sea surface.

*Presented at the symposium on Mathematical Modelling and Oceanic Studies, 70th Session of Indian Science Congress, Tirupathi, 3-8 Jan. 1983.

$$\frac{\partial \bar{u}}{\partial t}+\frac{\partial(u\bar{u})}{\partial x}+\frac{\partial}{\partial y}(v\bar{u})-f\bar{v}$$

$$=-g(\zeta+h)\frac{\partial \zeta}{\partial x}+\frac{\tau_x^{\zeta}}{\rho_w}-\frac{k\bar{u}}{(\zeta+h)}\left[\frac{\bar{u}^2}{(\zeta+h)^2}+\frac{\bar{v}^2}{(\zeta+h)^2}\right]^{1/2} \quad \ldots(4)$$

$$\frac{\partial \bar{v}}{\partial t}+\frac{\partial}{\partial x}(u\bar{v})+\frac{\partial}{\partial y}(v\bar{v})+f\bar{u}$$

$$=-g(\zeta+h)\frac{\partial \zeta}{\partial y}+\frac{\tau_y^{\zeta}}{\rho_w}-\frac{k\bar{v}}{(\zeta+h)}\left[\frac{\bar{u}^2}{(\zeta+h)^2}+\frac{\bar{v}^2}{(\zeta+h)^2}\right]^{1/2} \quad \ldots(5)$$

where $\bar{u}$ and $\bar{v}$ are prognostic variables defined by

$\bar{u}=u(\zeta+h)$ or $u=\bar{u}/(\zeta+h)$

$\bar{v}=v(\zeta+h)$ or $v=\bar{v}/(\zeta+h)$

The surface wind stress components in Eqs 4 and 5 are given by

$$\tau_x^{\zeta}=C_D\rho_a|V_a|u_a \quad \ldots(6)$$

$$\tau_y^{\zeta}=C_D\rho_a|V_a|v_a \quad \ldots(7)$$

Where V_a is the scalar wind $(u_a^2+v_a^2)^{1/2}$ at 10 m above sea surface and u_a and v_a are the components of V_a to the east and north respectively and C_D is the non-dimensional coefficient which is taken as 2.8×10^{-3} in the numerical experiments.

The following assumptions are made in deriving Eqs 3 to 5:

(i) Hydrostatic balance is maintained along the vertical; (ii) atmospheric pressure gradient at sea surface is ignored; (iii) non-linear advective terms in horizontal momentum equations are important; (iv) fluid density is horizontally uniform; and (v) bottom friction is directly related to the components of depth averaged velocity.

Assumptions (i) and (iv) are fairly valid in view of scales of motions considered in the present study. The non-linear advective terms in Eqs 1 and 2 usually make substantial contribution as the area of investigation is highly variable in depth. Assumption (v) can be questioned as vertical variation in the flow caused by vertical variation in stratification significantly affect the bottom stress. In models of this kind, the bottom stress is normally parametrised in terms of depth averaged velocity components.

Boundary and initial conditions—Open sea boundary condition: For purely wind-driven flow, the condition $\zeta=0$ along the open sea boundary may be used especially if the sea is shallow and its open sea boundary contiguous with deep ocean[3]. In the present model, a radiation type of boundary condition is used. Various such types of radiation conditions have been discussed by Flather and Heeps[7,13]. Here, internally generated wave energy is allowed to be transmitted outwards across the open sea boundary. Thus, in the present model the following radiation type boundary conditions is applied at the southern part of the model domain[11].

$$\left(v+\frac{g}{h}\right)^{1/2}\zeta=0 \text{ at } y=0 \quad \ldots(8)$$

Coastal or solid boundaries: In coastal and solid boundaries, the normal component of depth averaged flow should be zero. Thus, $v=0$ on those straight line boundary segments parallel to x-axis and $u=0$ on those lines parallel to y-axis (Fig. 2).

Initial condition is a state of rest or $u=v=\zeta=0$ at $t=0$.

Computation—Eqs 3 to 5 are solved subject to the above boundary and initial conditions by means of an explicit finite difference scheme. The Grid system, bathymetry and area (long. 80°-99°E; lat. 6°-22.5°N) chosen to cover the Bay of Bengal are same as that used by Johns *et al.*[11] In the x-y plane, there are 3 distinct types of computational points. With i even and j odd the point is ζ point at which ζ is computed (x, Fig. 1). If i is odd and j is odd, the point is u point at which u is computed. (0, Fig. 1). If i is even and j is even, the point is v point at which v is computed (Δ, Fig. 1). All variables corresponding to i,jth element are denoted with a subscript i,j(e.g.u_{ij}).

Finite difference approximation to the basic Eqs 3 to 5 may be written as

$$\frac{\zeta_{i,j}^{p+1}-\zeta_{i,j}^{p}}{\Delta t}=\left[\frac{\bar{u}_{i+1,j}^{p}-\bar{u}_{i-1,j}^{p}}{2\Delta x}+\frac{\bar{v}_{i,j+1}^{p}-\bar{v}_{i,j-1}^{p}}{2\Delta y}\right] \quad \ldots(9)$$

$$\frac{\bar{u}_{i,j}^{p+1}-\bar{u}_{i,j}^{p}}{\Delta t}+\frac{(u\bar{u})_{i+2,j}^{p}-(u\bar{u})_{i-2,j}^{p}}{4\Delta x}$$

$$+\frac{(v\bar{u})_{i,j+1}^{p}-(v\bar{u})_{i,j-1}^{p}}{2\Delta y}-f_{i,j}\bar{\bar{v}}_{i,j}^{p}$$

$$=-g(\zeta+h)_{i,j}^{p+1}\left[\frac{\zeta_{i+1,j}^{p+1}-\zeta_{i-1,j}^{p+1}}{2\Delta x}\right]+\frac{\tau_x^{\zeta}}{\rho_w}$$

$$\frac{-k\bar{u}_{i,j}^{p+1}}{(\zeta+h)_{i,j}^{p+1}}\left[\frac{\bar{u}_{i,j}^{2p}}{(\zeta+h)_{i,j}^{2}}+\frac{\bar{\bar{v}}_{i,j}^{2p}}{(\zeta+h)_{i,j}^{2}}\right]^{1/2} \quad \ldots(10)$$

$$\frac{\bar{v}_{i,j}^{p+1}-\bar{v}_{i,j}^{p}}{\Delta t}+\frac{(u\bar{v})_{i+1,j}^{p}-(u\bar{v})_{i-1,j}^{p}}{2\Delta x}$$

$$+\frac{(v\bar{v})_{i,j+2}^{p}-(v\bar{v})_{i,j-2}^{p}}{4\Delta y}+f_{i,j}\tilde{\bar{u}}_{i,j}^{p+1}$$

$$=-g(\zeta+h)_{i,j}^{p+1}\left[\frac{\zeta_{i,j+1}^{p+1}-\zeta_{i,j-1}^{p+1}}{2\Delta y}\right]+\frac{\tau_y^{\zeta}}{\rho_w}$$

$$\frac{-k\bar{v}_{i,j}^{p+1}}{(\zeta+h)_{i,j}^{p+1}}\left[\frac{\bar{u}_{i,j}^{2p}}{(\zeta+h)_{i,j}^{2}}+\frac{\bar{v}_{i,j}^{2p}}{(\zeta+h)_{i,j}^{2}}\right]^{1/2} \quad \ldots(11)$$

where

$$\tilde{\bar{u}}_{i,j}=\frac{1}{4}(\bar{u}_{i+1,j+1}+\bar{u}_{i+1,j-1}+\bar{u}_{i-1,j+1}+\bar{u}_{i-1,j-1})$$

$$\tilde{\bar{v}}_{i,j}=\frac{1}{4}(\bar{v}_{i+1,j+1}+\bar{v}_{i+1,j-1}+\bar{v}_{i-1,j+1}+\bar{v}_{i-1,j-1})$$

The elevation ζ at $j=1$ is determined from Eq. 8 which can be written in the difference form as follows:

$$\frac{1}{2}\left[\frac{g}{h_{i,2}}\right]^{1/2}\left[\zeta_{i,1}^{p+1}+\zeta_{i,3}^{p+1}\right]+v_{i,2}^{p}=0 \quad \ldots(12)$$

Thus it leads to an updating procedure for the elevation on the southern open sea boundary.

Eq. 9 to 11 taken in order may be solved with appropriate boundary and initial conditions as already mentioned to determine $\zeta_{i,j}u_{i,j}$ and $v_{i,j}$ respectively at future time step $(p+1)$ from known values at the earlier time step p, thereby advancing the solution by one step. As we are mainly interested in computing the resultant current speed and direction at a particular grid point, v values are interpolated at u points for each time step by averaging the v values using the relation

$$v_{i,j}=\frac{1}{4}(v_{i+1,j+1}+v_{i-1,j+1}+v_{i+1,j-1}+v_{i-1,j-1}) \quad \ldots(13)$$

The resultant velocity and direction at the grid point for each time step are computed using the following two relations.

$$V_{i,j}=\sqrt{v_{i,j}^2+u_{i,j}^2} \quad \ldots(14)$$

$$\theta_{i,j}=\tan^{-1}\left(\frac{v_{i,j}}{u_{i,j}}\right) \quad \ldots(15)$$

This iterative procedure is carried out for the desired number of time steps starting from an initial state of rest.

In the finite difference approximations to Eqs 10 and 11, the following general remarks can be made about the discretisations. The pressure gradient terms in Eqs 10 and 11 are evaluated at the forward time level. This is possible explicitly using the value of ζ previously updated by the application of Eq. 9. It ensures computational stability subject to the time step being limited by space increment and gravity wave speed. In Eq. 10, the coriolis term is calculated explicitly at the previous time step whereas in Eq. 11 it is evaluated at the formal time level using the previously updated value of u.

Results and Discussion

Numerical experiments have been conducted using the analysis area. The grid spacing is uniform with $\Delta x = 33$ km and $\Delta y = 36.5$ km. The idealised bathymetry used in the model for wind-driven circulation is a shallow water depth of 10 m near the coastline and a maximum depth of 500 m at the central part of the Bay of Bengal. There are 59 points in the x-direction and 50 in the y-direction. Throughout the numerical experiments, $g = 9.81\ \text{m.sec}^{-2}$ and $\rho_w = 1\times10^6\ \text{g.m}^{-3}$ are taken as constant. The time step is chosen to satisfy the Courant Friedrich's Lewy stability criterion[3] given by $\Delta t < \min(\Delta x, \Delta y)(2gh)^{-1/2}$. A time step of 180 sec is chosen for the numerical integration which satisfied the above inequality.

Wind-stress at sea surface due to a constant wind of $10\ \text{m.sec}^{-1}$ and direction 225° is calculated using the Eqs 6 and 7. During the southwest monsoon, winds normally blow from SW direction with speed ranging from 8 to $15\ \text{m.sec}^{-1}$. Hence, in these numerical experiments, the choice of wind speed of $10\ \text{m.sec}^{-1}$ blowing from the SW direction in representative of SW monsoon. Hence, the general pattern of wind-driven circulation for the same period over the Bay of Bengal could be studied.

In the numerical experiments, an initial state of rest is prescribed and the governing equations ahead in time for a period of 100 h are integrated. Results (Fig. 2) refer to wind-driven circulation generated by constant wind speed and direction after 15, 30 and 60 h of numerical integrations. A steady circulation and sea surface height are established after maintaining steady wind for 50 h. As anticipated, maximum current speed is observed near the coastal region where a maximum speed of $30\ \text{cm.sec}^{-1}$ is observed during the steady state. In the central part of the Bay, current is generally weak and is of the order of 1 to $5\ \text{cm.sec}^{-1}$ even after 60 h of numerical integration. One interesting aspect of the model circulation is that 2 branches of circulation are formed at the central part of the Bay. One branch flows northwards along the east coast of India and

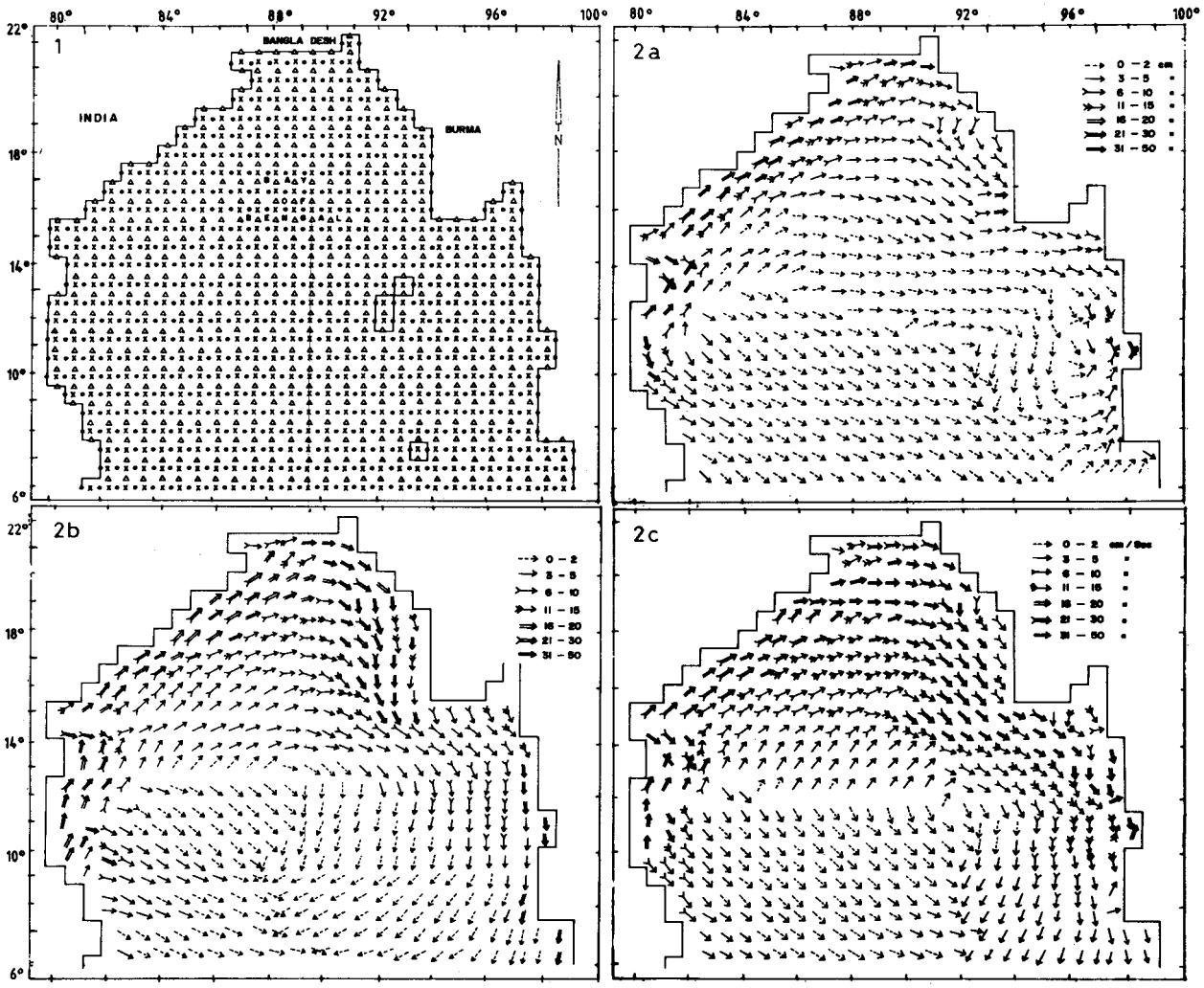

Fig. 1—Finite difference mesh for the model [Points 0, Δ and x are u, v and ζ points respectively]

Fig. 2—Wind-driven circulation generated by a constant wind field (speed 10 m.sec^{-1} and direction 225°TN) after (a) 15 (b) 30 and (c) 60 h of numerical integration of the model

returns towards south through the eastern part of the model domain (Fig. 2) like a clockwise circulation while the other branch flows southeast from the central part of the Bay and meets the clockwise circulation from the northern side of model area. Thus, a clear divergence, though weak, is generated at the central part of the Bay which is to be examined in the future observational programmes. From the model experiments, it is clear that the coastal configuration also affects the circulation. This is due to the reflection of water from the coastal walls which are represented as straightline orthogonal segments in the model.

The peculiarities of circulation as observed in the model can be explained in terms of the period of integration of the model equations and idealised bathymetry used in the model. As the wind stress is uniform throughout the model area, the divergence in the central part of the Bay cannot be attributed to wind shear stress. Heaps[13] has commented on the remarkable influence of bathymetry on the current pattern in his model of Irish Sea. In the present model also, the current patterns more or less follow the bottom contours. This type of behaviour is observed in the well known homogeneous ocean circulation theory[12] in which the flow tends to follow the contours of f/h where f is the coriolis parameter and h is the water depth. Our contention is that the combined effects of idealised bathymetry used in the model along with period of integration might have contributed to the emergence of a clear divergence in the central part

of the Bay of Bengal. For a better reproduction of circulation in the Bay, realistic bathymetry, windfield and the chain of islands in the Bay of Bengal should be taken into account.

Acknowledgement

The authors express their thanks to the scientists of the Physical Oceanography Division for their constructive comments on this paper. One of the authors (NB) expresses his gratitude to Prof. M P Singh, head, CAFS and other scientists of the Centre for Atmospheric and Fluid Sciences, IIT, New Delhi for useful discussions and other facilities.

References

1 Lighthill M J, *Phil Trans Roy Soc London*, **A265** (1969) 45.

2 Cox M D, *Deep-Sea Res*, **17** (1970) 47.

3 Fandry C B, *Aust J Mar Freshwater Res*, **32** (1981) 9.

4 Heaps N S, *Phil Trans Roy Soc London*, **A265** (1969) 93.

5 Heaps N S, *Geophys J R Astr Soc*, **35** (1973) 99.

6 Heaps N S, *Development of a storm surge model at Bidston*, Institute of Ocean Sciences, Report No **53** (1977).

7 Flather R A, *Mem Soc R Sci Liege Vol Hors Sor*, **6** (1976) 141.

8 Flather R A & Heaps N S, *Geophys J R Astron Soc*, **42** (1976) 489.

9 Flather R A & Davies A M, *Quart J R Meteorol Soc*, **102** (1976) 123.

10 Martinsen E A, Jgevik B & Roed L P, *J Phys Oceanogr*, **9** (1979) 1126.

11 Johns B, Dube S K, Mohanty U C & Sinha P C, *Quart J R Meteorol Soc*, **107** (1981) 919.

12 Kamenkovich V M, *Tr Inst Oceanol Akad Hauk SSSR*, **56** (1962) 241.

13 Reaps N S, Rapp P V, *Reun Cons Int Explor Mer*, **167** (1974) 147.